Temperature driven dynamical arrest of a network fluid: the role of loops

C. S. Dias,[1,2,*] J. M. Tavares,[2,3,†] N. A. M. Araújo,[1,2,‡] and M. M. Telo da Gama[1,2,§]

[1] *Departamento de Física, Faculdade de Ciências, Universidade de Lisboa, 1749-016 Lisboa, Portugal*
[2] *Centro de Física Teórica e Computacional, Universidade de Lisboa, 1749-016 Lisboa, Portugal*
[3] *Instituto Superior de Engenharia de Lisboa, ISEL, Avenida Conselheiro Emídio Navarro, 1 1950-062 Lisboa, Portugal*

Low-density networks of molecules or colloids are formed at low temperatures when the interparticle interactions are valence limited. Prototypical examples are networks of patchy colloids, where the limited valence results from highly directional pairwise interactions. We combine extensive Langevin simulations and Wertheim's theory of association to study these networks. A temperature driven crossover was observed from exponential to scale-free relaxation dynamics. The exponent of the latter is independent of temperature and initial configuration. This crossover stems from the formation of a dynamically arrested percolating gel, with a number of loops, compromising the feasibility of observing thermodynamic structures. Most notably, under conditions of equilibrium phase separation, an arrested gel of intermediate density forms and it is observed to age slowly. This contrasts with the dynamics of loopless gels, where such an arrest was not observed.

PACS numbers: 81.40.Cd,64.60.ah,64.75.Yz

arXiv:1604.05279v1 [cond-mat.soft] 18 Apr 2016

The formation of stable low-density arrangements of interconnected molecules or colloids is an open challenge that attracted researchers in the last decade [1–5]. These unique structures are simultaneously of low packing fraction and resilient to mechanical perturbations. The former can be achieved through limited valence of the individual constituents. The latter requires sufficiently strong interparticle bonding. However, establishing strong bonds leads to rough energy landscapes, challenging the formation of the final equilibrium structures [6, 7]. Kinetically arrested structures are usually obtained, which may be significantly different from the thermodynamic ones.

Colloidal valence may be engineered by chemically patterning the colloidal surfaces with attractive patches [9–19]. Studies of equilibrium phase diagrams have shown that for low valence, due to the decrease in the density of the liquid binodal, a gel-like low density structure is thermodynamically stable for intermediate attractive strengths [20]. For strong attractions, however, the system is expected to phase separate into colloid-rich and colloidal-poor phases [21–26]. Nevertheless, as the lifetime of thermal reversible bonds increases exponentially with the attraction an arrested gel is formed [7, 27], in line with experimental observations for mixtures of colloids and polymers [28]. These non-ergodic gels are significantly different from the thermodynamic ones.

In what follows we investigate the collective dynamics of limited-valence colloids in various regions of the phase diagram. We show that the interplay between relaxation mechanisms at different length and time scales leads to distinct dynamics at low and high temperatures. At high temperatures the dynamics is driven by sequences of bond breaking and forming events, and is characterized by an Arrhenius relaxation time related to the thermal reversibility of the bonds. At low temperatures, however, the dynamics involves concerted moves in a range of length and time scales, leading to scale-free aging of the kinetically arrested gel.

We consider a three-dimensional system of spherical colloids of diameter σ with three patches along the equator with an opening angle of $2\pi/3$. The core-core interaction is pairwise repulsive, described by the Yukawa potential $V_Y = \frac{A}{\alpha}\exp\left(-\alpha\left[r-\sigma\right]\right)$, where A is the strength of the potential, r is the distance between the colloids centers, and α^{-1} is the range of interaction. The short-range patch-patch attraction is described by an inverse Gaussian potential, $V_G = -\varepsilon\exp(-r_p^2/\xi^2)$, where ε is the strength of attraction, $\xi = 0.1\sigma$ the width of the Gaussian, and r_p is the patch-patch distance. For simplicity, patch-colloid interactions are neglected. To follow the collective dynamics, we integrate the corresponding Langevin equations for the translational and rotational motions (see Supplemental Material for further details [8]).

Figure 1 shows the temperature dependence of the bonding fraction, p_b, defined as the fraction of patches that are bonded. The squares are asymptotic values extrapolated from the numerical data. The solid (red) line corresponds to the equilibrium value as predicted by Wertheim's first-order perturbation theory (details in the Supplemental Material [8]). While at high temperatures the numerical results are in line with the equilibrium results, at low temperatures the bonding fraction is systematically lower than the equilibrium value and does not converge to unity at zero temperature. This signals the presence of an arrested gel in the coexistence region (see snapshots in Fig. 1 and Supplemental Material for the equilibrium phase diagram [8]). Note that the numerical data are the asymptotic values, suggesting that

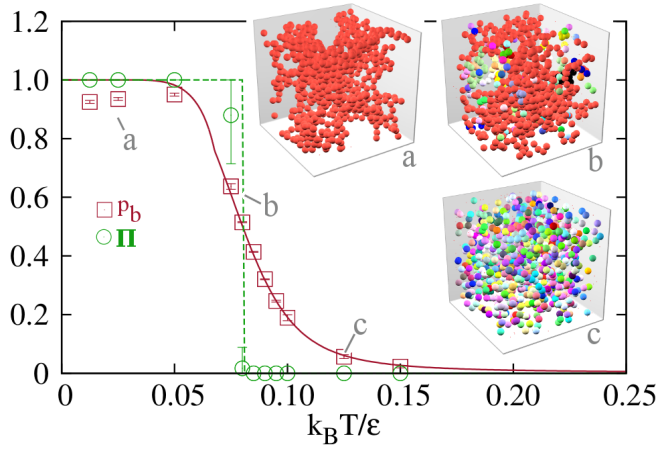

FIG. 1. The (red) squares are the bonding fraction p_b as a function of the rescaled temperature k_BT/ε, obtained from the asymptotic extrapolation of the numerical data. The solid line is the equilibrium value predicted by Wertheim's first-order perturbation theory of association (see Supplemental Material for further details [8]). The (green) circles are the wrapping probability Π, defined numerically as the fraction of samples with an aggregate of bonded colloids that simultaneously touches the top and bottom boundaries of the simulation box. The dashed line corresponds to the mean-field prediction, which is a step function at k_BT^*/ε, where $p_b(k_BT^*/\varepsilon) = 1/2$. Insets are snapshots for k_BT/ε of a) 0.025, b) 0.075, and c) 0.125, where different colors correspond to different aggregates of connected particles. Numerical results were obtained by averaging over 10 samples, of a box of linear size $L = 16$, in units of the particle diameter, with $N = 800$ colloidal particles.

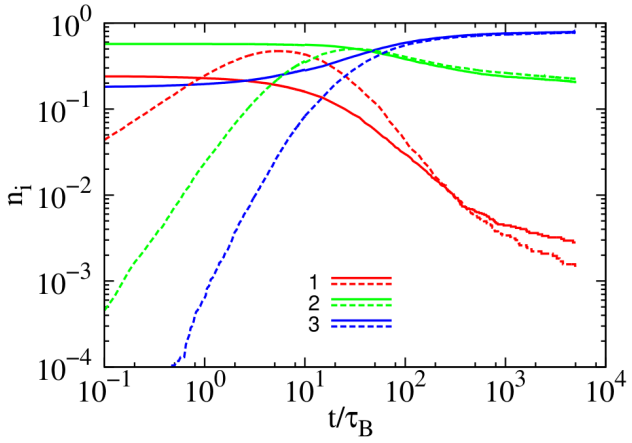

FIG. 2. Time evolution of the fraction of colloids with one (red), two (green), and three bonds (blue), at $k_BT/\varepsilon = 0.025$. The solid lines are for the relaxation of a tree-like gel grown by ballistic aggregation and loopless irreversible bond formation. The dashed lines are for the aggregation of an initial fully disconnected suspension of patchy colloids. Time is rescaled by the Brownian time $\tau_B = \sigma^2/D_t$, where σ is the colloid diameter and D_t its diffusion coefficient. Results are averages over 100 samples for $t/\tau_B < 10$ and and 10 samples for $t/\tau_B > 10$, of a cubic box of length $L = 16$, in units of particle diameter.

the thermodynamic structures are not accessible.

Far-from-equilibrium the asymptotic structures depend on the dynamics. We have considered two limiting initial configurations with the same number of particles: A tree-like gel (single aggregate) and a fully disconnected suspension. The former was grown by ballistic aggregation and loopless irreversible bond formation [29] and corresponds to relaxing a low-temperature structure [30]. The latter is equivalent to quenching a colloidal solution from a much higher temperature. No dependence of the bonding fraction on the initial configuration was observed. Within error bars, the asymptotic value of p_b is the same, even if an arrested gel is formed, and differs from the thermodynamic value. Figure 2 shows the time evolution of the fraction of colloids with one (n_1), two (n_2), and three bonds (n_3) for both initial configurations at $k_BT/\varepsilon = 0.025$. When starting from a tree-like gel, n_3 increases monotonically, while n_1 and n_2 decrease, suggesting that structural relaxation is driven by loop formation through the maximization of bonded patches. When starting from a completely disconnected system, the kinetic pathway is significantly different, resembling a typical aggregation process. n_1 initially increases due to the formation of small, chain-like, aggregates but eventually peaks at an intermediate time, when branching and loop closing dominate. Note that, despite the significantly different kinetic pathways towards the asymptotic value, the final value is the same (within error bars) and differs from the thermodynamic one ($n_3 \approx 1$ and $n_1 < 10^{-10}$). This hints at much larger basins of attraction of the arrested states in the configuration manifold relative to the equilibrium ones. For low-valence loopless gels, it has been argued that relaxation corresponds to progressive cooling, such that time can be mapped to an effective temperature [34]. This is not what we observe here. As we show in the Supplemental Material [8], in the presence of loops, the fraction of colloids with one, two, and three bonds is different from the equilibrium ones for the same bonding fraction. Thus, the evolution of the gel does not correspond to a succession of equilibrium configurations.

To characterize the dynamics, we follow the convergence of p_b to the asymptotic value $p_b(\infty)$ (see Fig. 3). When equilibrium is accessible (Fig. 3(a)), the convergence is exponential, with a characteristic relaxation time that also scales exponentially with the reduced temperature (see Fig. 3(c)). This suggests that relaxation is driven by a sequence of thermally activated bond breaking and formation. By contrast, in the coexistence region, p_b follows a power law in time, with an exponent of 0.6 ± 0.1 (Fig. 3(b)). The numerical data is consistent with the same exponent for different initial conditions

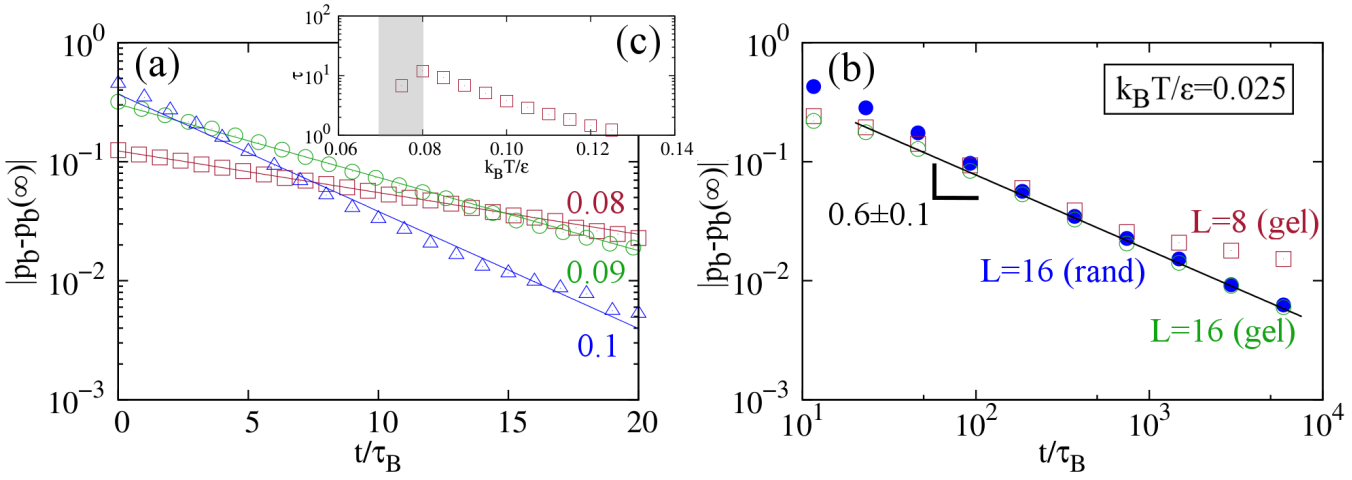

FIG. 3. Convergence of the bonding fraction to the asymptotic value $|p_b - p_b(\infty)|$ at (a) high temperature ($k_BT/\varepsilon > 0.075$) and (b) low temperature ($k_BT/\varepsilon < 0.075$), where the time is rescaled by the Brownian time $\tau_B = \sigma^2/D_t$, σ is the colloid diameter and D_t its diffusion coefficient. (c) Temperature dependence of the relaxation time τ given by $p_b \sim \exp(-t/\tau)$. The shadowed region corresponds to the critical window where strong finite size effects are observed as well as the Kovacs effect (see Supplemental Material [8]). Numerical results were obtained by averaging over 10 samples at low temperature and 100 samples at high temperature, in a box of length $L = \{8, 16\}$, in units of particle diameter.

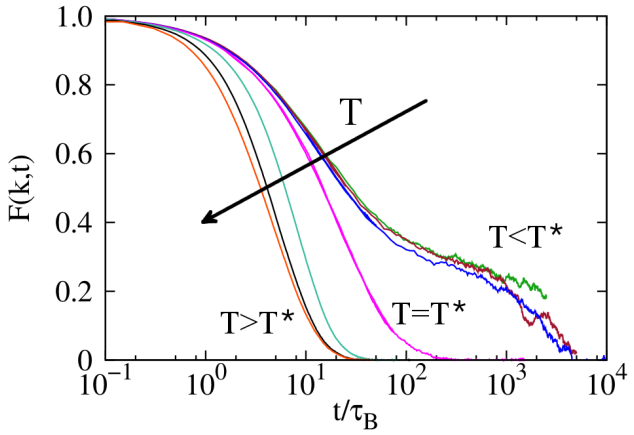

FIG. 4. Intermediate scattering function $F(k,t)$ at $k = \pi/(2\sigma)$ starting from a low temperature gel at temperatures $k_BT/\varepsilon = \{0.0125, 0.025, 0.05, 0.075, 0.1, 0.125, 0.15\}$. Numerical results were obtained by averaging over 10 samples at low temperatures and 100 samples at high temperatures, in a box of length $L = 16$, in units of the particle diameter.

(tree-like gel and fully disconnected) and temperatures in the coexistence region (see Supplemental Material [8]).

Figure 4 shows the time evolution of the intermediate scattering function $F(\mathbf{k}, t)$, defined as,

$$F(\mathbf{k},t) = \frac{1}{N}\langle \sum_j^N \exp\left[i\mathbf{k}\cdot(\mathbf{r}_j(t) - \mathbf{r}_j(0))\right]\rangle, \qquad (1)$$

where $\mathbf{r}_j(t)$ is the position of particle j at time t and $\mathbf{k}$ is the wave number. We consider the intermediate value $k = \pi/(2\sigma)$. At high temperatures, the intermediate scattering function decays exponentially in time. At low temperatures, a plateau is observed due to the presence of an arrested gel. Studies of gel dynamics based on numerical simulations and mode coupling theory suggest power-law scaling of the intermediate scattering function before and after the plateau [31–33]. These power laws indicate the lack of a characteristic decorrelation time in the individual particle positions. The formation of new bonds in the arrested gel is mediated by the collective rearrangement of colloids on many scales and therefore it also lacks a characteristic time.

At low temperatures aging is drastically different from that predicted for loopless gels [34, 35]. Studies combining Smoluchowski equations and either event driven Molecular Dynamics or Brownian dynamics predict accessible equilibrium structures and characteristic relaxation times [30, 35–38]. This hints at a key role of the loops on the overall dynamics. The presence of loops hinders effectively the relaxation of the structures and slows down the dynamics. Singly connected branches can relax by breaking thermally reversible bonds followed by diffusion and formation of new bonds. In the presence of loops, typically, there are redundant connections of each branch to the macroscopic aggregate and when a bond is broken the relaxation of the entire branch is constrained by the bonds, thus affecting the overall dynamics.

In summary, we studied the dynamics of colloids with limited valence in different regions of the phase diagram. At low densities, crowding effects are absent even at low temperatures (or strong interparticle attraction). How-

ever, arrested gels are formed in the coexistence region due to the slow thermal-reversibility of bonds. Such long-living bonds induce structural disorder that is quenched on the experimental timescale effectively hindering the relaxation of the colloidal structure towards thermodynamic equilibrium. As a consequence, a temperature driven transition in the dynamics is observed. At high temperatures (or weak interparticle attraction) the relaxation dynamics is driven by sequences of individual bond breaking and re-bonding, and thus the approach to equilibrium is exponential with a characteristic Arrhenius time. By contrast, when the arrested gel is formed, the relaxation involves collective rearrangements at different length- and timescales and a scale-free relaxation (aging) of the gel is observed. The asymptotic configuration is independent of the initial configuration, but significantly different from the thermodynamic one.

The numerical data for gel aging in the coexistence region is consistent with a universal exponent, $0.6 \pm 0.1 (\approx 2/3)$, for the evolution of the bonding fraction. A theoretical justification for this exponent is still missing. Aging is not observed for loopless gels, suggesting that loops play an important role in the slowing down of the relaxation dynamics. Numerical studies of network fluids of colloids with (two) oppositely oriented dipole moments suggest a power-law decay of the bond correlation function [39, 40]. These results, obtained by Monte Carlo (equilibrium) simulations, are not related to the real dynamics, but hint at a dynamic slowing down driven by gel formation. It would be interesting to investigate the dynamics of these dipolar systems and to compare their aging to that reported here.

Previous studies of gels focused on a geometrical characterization based on the aggregate-size distribution [41, 42]. A mapping to percolation, assuming that aggregates decay exponentially in time, with a relaxation time that is an algebraic function of the their size, predicts an evolution of the time correlation function near the sol-gel transition, which is a power law only at threshold. In the sol and gel phases, the (time) correlation function is the product of a power law and a stretched exponential. By contrast, we observed the evolution of a single aggregate and found no evidence of coarsening or domain growth. In addition, we found that the bonding fraction of the gel evolves as a power law (everywhere) in the coexistence region, with an exponent which differs from the coarsening one.

Finally, there is the question of the dependence of the dynamics on the colloidal valence. At low valence, crowding effects are absent. However, the network density increases with valence [43–46] and as the valence increases, crowding effects are expected to play a role. Khalil *et al.* investigated structural arrest transitions in polymer suspensions with cross linkers [47], a problem that may be related to limited valence mixtures of colloids. An interplay between the glass and gel transitions was observed depending on the polymer and cross-linker concentrations. Future work could address similar questions in network fluids and/or mixtures as a function of their valence.

We acknowledge fruitful discussions with Emanuela Del Gado and financial support from the Portuguese Foundation for Science and Technology (FCT) under Contracts nos. EXCL/FIS-NAN/0083/2012, UID/FIS/00618/2013, and IF/00255/2013.

* csdias@fc.ul.pt
† jmtavares@fc.ul.pt
‡ nmaraujo@fc.ul.pt
§ mmgama@fc.ul.pt

[1] J. Dobnikar, A. Snezhko, and A. Yethiraj, Soft Matt. **9**, 3693 (2013).
[2] E. Zaccarelli, J. Phys.: Condens. Matter **19**, 323101 (2007).
[3] S. L. Elliott, R. J. Butera, L. H. Hanus, and N. J. Wagner, Faraday discuss. **123**, 369 (2003).
[4] B. Ruzicka, E. Zaccarelli, L. Zulian, R. Angelini, M. Sztucki, A. Moussaïd, T. Narayanan, and F. Sciortino, Nature Mater. **10**, 56 (2011).
[5] F. Sciortino, S. Mossa, E. Zaccarelli, and P. Tartaglia, Phy. Rev. Lett. **93**, 055701 (2004).
[6] D. Chakrabarti, H. Kusumaatmaja, V. Rühle, and D. J. Wales, Phys. Chem. Chem. Phys. **16**, 5014 (2014).
[7] E. Zaccarelli, I. Saika-Voivod, S. V. Buldyrev, A. J. Moreno, P. Tartaglia, and F. Sciortino, J. Chem. Phys. **124**, 124908 (2006).
[8] See Supplemental Material at , which includes Refs. [48–56].
[9] J. Zhang, E. Luijten, and S. Granick, Ann. Rev. Phys. Chem. **66**, 581 (2015).
[10] J. A. Paulson, A. Mesbah, X. Zhu, M. C. Molaro, and R. D. Braatz, J. Proc. Cont. **27**, 38 (2015).
[11] P. J. Lu and D. A. Weitz, Annu. Rev. Condens. Matter Phys. **4**, 217 (2013).
[12] E. Duguet, A. Désert, A. Perro, and S. Ravaine, Chem. Soc. Rev. **40**, 941 (2011).
[13] J. Hu, S. Zhou, Y. Sun, X. Fang, and L. Wu, Chem. Soc. Rev. **41**, 4356 (2012).
[14] I. Kretzschmar and J. H. Song, Curr. Op. Coll. Interf. Sci. **16**, 84 (2011).
[15] S. Sacanna and D. J. Pine, Curr. Op. Coll. Interf. Sci. **16**, 96 (2011).
[16] M. J. Solomon, Curr. Op. Coll. Interf. Sci. **16**, 158 (2011).
[17] A. B. Pawar and I. Kretzschmar, Macromol. Rapid Commun. **31**, 150 (2010).
[18] S. Sacanna, D. J. Pine, and G.-R. Yi, Soft Matt. **9**, 8096 (2013).
[19] V. N. Manoharan, Science **349**, 1253751 (2015).
[20] E. Zaccarelli, S. V. Buldyrev, E. La Nave, A. J. Moreno, I. Saika-Voivod, F. Sciortino, and P. Tartaglia, Phys. Rev. Lett. **94**, 218301 (2005).
[21] N. A. Mahynski and A. Z. Panagiotopoulos, J. Chem. Phys. **142**, 074901 (2015).
[22] E. G. Noya and E. Bianchi, J. Phys.: Cond. Matt. **27**, 234103 (2015).

[23] F. Romano, J. Russo, and H. Tanaka, Phy. Rev. Lett. **113**, 138303 (2014).
[24] J. Russo, P. Tartaglia, and F. Sciortino, J. Chem. Phys. **131**, 014504 (2009).
[25] E. Bianchi, J. Largo, P. Tartaglia, E. Zaccarelli, and F. Sciortino, Phy. Rev. Lett. **97**, 168301 (2006).
[26] E. Bianchi, R. Blaak, and C. N. Likos, Phys. Chem. Chem. Phys. **13**, 6397 (2011).
[27] K. Kroy, M. E. Cates, and W. C. K. Poon, Phys. Rev. Lett. **92**, 148302 (2004).
[28] S. Manley, H. M. Wyss, K. Miyazaki, J. C. Conrad, V. Trappe, L. J. Kaufman, D. R. Reichman, and D. A. Weitz, Phys. Rev. Lett. **95**, 238302 (2005).
[29] C. S. Dias, N. A. M. Araújo, and M. M. Telo da Gama, J. Chem. Phys. **139**, 154903 (2013).
[30] F. Sciortino, C. De Michele, S. Corezzi, J. Russo, E. Zaccarelli, and P. Tartaglia, Soft Matt. **5**, 2571 (2009).
[31] A. Coniglio, A. de Candia, T. Abete, A. Fierro, M. Pica Ciamarra, E. Del Gado, and R. Pastore, in *Proceedings of the International School of Physics "Enrico Fermi"*, edited by H. E. S. Francesco Mallamace (IOS Press, Varenna, 2012) p. 55.
[32] E. Del Gado, A. Fierro, L. de Arcangelis, and A. Coniglio, Europhys. Lett. **63**, 1 (2003).
[33] A. Fierro, T. Abete, and A. Coniglio, J. Chem. Phys. **131**, 194906 (2009).
[34] F. Sciortino and E. Zaccarelli, Curr. Op. Coll. Interf. Sci. **15**, 246 (2011).
[35] S. Corezzi, D. Fioretto, and F. Sciortino, Soft Matt. **8**, 11207 (2012).
[36] S. Corezzi, D. Fioretto, C. De Michele, E. Zaccarelli, and F. Sciortino, J. Phys. Chem. B **114**, 3769 (2010).
[37] S. Corezzi, C. De Michele, E. Zaccarelli, D. Fioretto, and F. Sciortino, Soft Matt. **4**, 1173 (2008).
[38] S. Corezzi, C. De Michele, E. Zaccarelli, P. Tartaglia, and F. Sciortino, J. Phys. Chem. B **113**, 1233 (2009).
[39] H. Schmidle, S. Jäger, C. K. Hall, O. D. Velev, and S. H. L. Klapp, Soft Matt. **9**, 2518 (2013).
[40] S. H. L. Klapp, Curr. Op. Coll. Interf. Sci. **21**, 76 (2016).
[41] A. Coniglio, J. J. Arenzon, A. Fierro, and M. Sellitto, Eur. Phys. J. Special Topics **223**, 2297 (2014).
[42] H. Löwe, P. Müller, and A. Zippelius, J. Phys.: Condens. Matter **17**, S1659 (2005).
[43] D. J. Kraft, J. Hilhorst, M. A. P. Heinen, M. J. Hoogenraad, B. Luigjes, and W. K. Kegel, J. Phys. Chem. B **115**, 7175 (2011).
[44] M. Sabapathy, S. D. Christdoss Pushpam, M. G. Basavaraj, and E. Mani, Langmuir **31**, 1255 (2015).
[45] N. Kern and D. Frenkel, J. Chem. Phys. **118**, 9882 (2003).
[46] C. S. Dias, N. A. M. Araújo, and M. M. Telo da Gama, Mol. Phys. **113**, 1069 (2015).
[47] N. Khalil, A. de Candia, A. Fierro, M. P. Ciamarra, and A. Coniglio, Soft Matt. **10**, 4800 (2014).
[48] C. S. Dias, C. Braga, N. A. M. Araújo, and M. M. Telo da Gama, Soft Matt. **12**, 1550 (2016).
[49] O. A. Vasilyev, B. A. Klumov, and A. V. Tkachenko, Phys. Rev. E **88**, 012302 (2013).
[50] S. Plimpton, J. Comp. Phys. **117**, 1 (1995).
[51] M. G. Mazza, N. Giovambattista, H. E. Stanley, and F. W. Starr, Phys. Rev. E **76**, 031203 (2007).
[52] F. Sciortino, E. Bianchi, J. F. Douglas, and P. Tartaglia, J. Chem. Phys. **126**, 194903 (2007).
[53] J. A. Barker and D. Henderson, J. Chem. Phys. **47**, 4714 (1967).
[54] M. S. Wertheim, J. Chem. Phys. **85**, 2929 (1986).
[55] S. Mossa and F. Sciortino, Phys. Rev. Lett. **92**, 045504 (2004).
[56] A. J. Kovacs, J. J. Aklonis, J. M. Hutchinson, and A. R. Ramos, J. Polym. Sci. Part B **17**, 1097 (1979).

Supplemental Material: Temperature driven dynamical arrest of a network fluid: the role of loops

C. S. Dias,[1,2,*] J. M. Tavares,[2,3,†] N. A. M. Araújo,[1,2,‡] and M. M. Telo da Gama[1,2,§]

[1] *Departamento de Física, Faculdade de Ciências, Universidade de Lisboa, 1749-016 Lisboa, Portugal*

[2] *Centro de Física Teórica e Computacional, Universidade de Lisboa, 1749-016 Lisboa, Portugal*

[3] *Instituto Superior de Engenharia de Lisboa, ISEL, Avenida Conselheiro Emídio Navarro, 1 1950-062 Lisboa - Portugal*

MODEL

We consider spherical colloidal particles, all of the same size, with three equal patches distributed along the equator. The core-core interaction is repulsive, described by a Yukawa potential,

$$V_Y(r) = \frac{A}{\alpha}\exp\left(-\alpha\left[r-\sigma\right]\right), \tag{S1}$$

where σ is the diameter of the colloidal particles, $A/(\alpha k_B T) = 0.25$ is the interaction strength and $\alpha/\sigma = 0.4$ the inverse of the screening length. The core-core interaction is truncated at a cutoff distance $r_c = 1.5\sigma$ (for $r = r_c$ the potential is $10^{-9}A/\sigma$). The patch-patch interaction is described by an attractive inverted Gaussian potential [1, 2],

$$V_G(r_p) = -\varepsilon\exp(-r_p^2/\xi^2), \tag{S2}$$

where ε is the strength of attraction, $\xi = 0.1\sigma$ the width of the Gaussian, and r_p is the patch-patch distance. This interaction is truncated also at a cutoff distance $r_{pc} = \sigma$. For this set of parameters, we expect at most one bond per patch.

To resolve the stochastic trajectories of the particles, we integrate the corresponding Langevin equations of motion for the translational degrees of freedom,

$$m\dot{\vec{v}}(t) = -\nabla_{\vec{r}}V(\vec{r}) - \frac{m}{\tau_t}\vec{v}(t) + \sqrt{\frac{2mk_BT}{\tau_t}}\vec{\xi}(t), \tag{S3}$$

and the rotational ones,

$$I\dot{\vec{\omega}}(t) = -\nabla_{\vec{\theta}}V(\vec{\theta}) - \frac{I}{\tau_r}\vec{\omega}(t) + \sqrt{\frac{2Ik_BT}{\tau_r}}\vec{\xi}(t). \tag{S4}$$

We use the velocity Verlet scheme with a time step $\Delta t = 1\times10^{-5}$, in units of the Brownian time (time to diffuse one particle diameter), and the Large-scale Atomic/Molecular Massively Parallel Simulator (LAMMPS) for efficient simulations [3]. $\vec{v}$ and $\vec{\omega}$ are the translational and angular velocities, m and I are the mass and inertia of the colloidal particles, V is the pairwise potential, and $\vec{\xi}(t)$ is the stochastic term drawn from a random distribution with zero mean. We consider the damping time for the translational motion,

$$\tau_t = \frac{m}{6\pi\eta R}. \tag{S5}$$

From the Stokes-Einstein-Debye relation [4],

$$\frac{D_r}{D_t} = \frac{3}{4R^2}, \tag{S6}$$

and thus the rotational damping time is $\tau_r = 10\tau_t/3$.

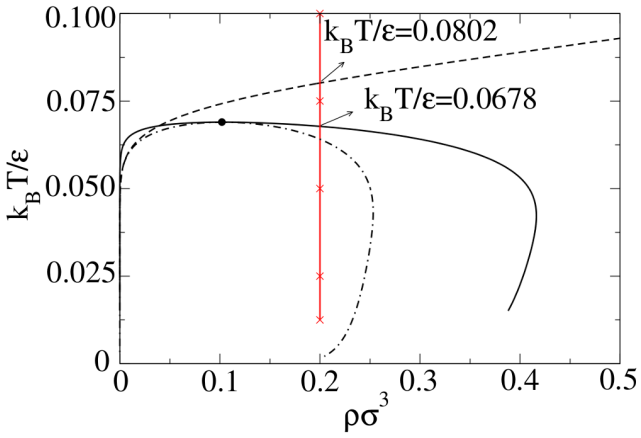

FIG. S1. Density-temperature phase diagram, where $\rho = N/V$ is the number of particles per unit volume and the temperature is the rescaled temperature k_BT/ε. The crosses are the simulated temperatures, the solid line is the binodal, the dashed line is the percolation line, and the dash-dotted line is the spinodal.

THEORY

The thermodynamic equilibrium properties of the model were calculated using Wertheim's first order perturbation theory (see, e.g. [5]). The Helmholtz free energy per particle f is the sum of a reference free energy f_{ref} and a perturbation (arising from bonding) f_b,

* csdias@fc.ul.pt
† jmtavares@fc.ul.pt
‡ nmaraujo@fc.ul.pt
§ mmgama@fc.ul.pt

$\beta f = \beta f_{ref} + \beta f_b$ where $\beta = 1/k_B T$. The reference potential was taken to be the repulsive Yukawa, $V_Y(r)$, and the perturbation (that promotes bonding) the attractive patch-patch interaction, $V_G(r_p)$. The bonding term is given by,

$$\beta f_b = n \ln(1 - p_b) - \frac{n}{2}(1 - p_b), \tag{S7}$$

where n is the number of (identical) patches ($n = 3$) and p_b is the bonding fraction, which in the thermodynamic limit corresponds to the fraction of bonded patches. We approximate f_{ref} by the hard sphere free energy (in the Carnahan-Starling approximation) of a system of particles with an effective diameter D calculated with the Barker-Henderson approximation [6],

$$D = \int_0^{+\infty} (1 - \exp\left[-\beta V_Y(r)\right]) \, dr. \tag{S8}$$

The probability p_b was calculated using the law of mass action,

$$p_b = n\rho\Delta(1 - p_b)^2, \tag{S9}$$

where ρ is the number density defined as the number of colloidal particles per unit volume. Δ is the integral of the Mayer function of the patch-patch interaction,

$$\Delta = \frac{1}{(4\pi)^2} \int d\vec{r} \int d\hat{r}_1 \int d\hat{r}_2 \left[\exp\left(-\beta V_G(r_p)\right] - 1\right) g_{ref}(r), \tag{S10}$$

where $\vec{r}$ is the vector between the centers of particles 1 and 2, and $\hat{r}_i$ is the unit vector that defines the position of a patch on particle i relative to the center of that particle. $g_{ref}(r)$ is the pair correlation function of the reference system, which is approximated by the contact value of the pair correlation function of a system of hard spheres of diameter D: $g_{ref}(r) = g_{HS}(r = D) = (1 - \eta/2)/(1 - \eta)^3$, with $\eta = \pi/6D^3\rho$. The multiple integral (S10) is then reduced to a sum of simple integrals through the following steps (a simple extension of Ref. [7]):

1 Define $z = r_p \equiv |\vec{r} + \sigma/2(\hat{r}_2 - \hat{r}_1)|$ and $x = |\vec{r} + \sigma/2\hat{r}_2|$.

2 Simplify (S10) using the change of variables: (i) from θ_1 to z^2, in the integration over $\hat{r}_1$, with $z^2 = x^2 + \sigma^2/4 - x\sigma\cos\theta_1$; (ii) from θ_2 to x^2, in the integration over $\hat{r}_2$, with $x^2 = r^2 + \sigma^2/4 - r\sigma\cos\theta_2$. One obtains,

$$\Delta = \frac{\pi g_{HS}(\eta)}{\sigma^2} \int_D^{+\infty} r dr \int_{(r-\sigma/2)^2}^{(r+\sigma/2)^2} \frac{dx^2}{x} \int_{(x-\sigma/2)^2}^{(x+\sigma/2)^2} f(z^2/\xi^2) dz^2, \tag{S11}$$

where $f(z^2/\xi^2) = \exp\left[-\beta V_G(z)\right] - 1$.

3 Change the order of integration in (S11), introducing a cut-off $z < \sigma$ (consistent with the procedure adopted in the simulations to define a bond) and distinguish the cases $D \geq \sigma$ and $D < \sigma$. After a simple but long calculation, Δ may be expressed as a sum of simple integrals. For $D \geq \sigma$,

$$\Delta = 4\pi\sigma^3 g_{HS}(\eta)\alpha^2 \int_{-\frac{\delta}{\alpha}}^{\frac{1}{\alpha}} y f(y) F_1(y, \alpha, \delta) dy, \tag{S12}$$

where $\alpha = \xi/\sigma$, $\delta = (\sigma - D)/\sigma$, and

$$F_1(y, \alpha, \delta) = \frac{\alpha^3 y^3}{6} + \frac{\alpha^2 y^2}{2} + \alpha y \delta \left(1 - \frac{\delta}{2}\right) + \delta^2 \left(\frac{1}{2} - \frac{\delta}{3}\right). \tag{S13}$$

For $D < \sigma$,

$$\Delta = 4\pi\sigma^3 g_{HS}(\eta)\alpha^2 \left(\Delta_1 + \Delta_2 + \Delta_3\right), \tag{S14}$$

where,

$$\Delta_1 = \int_0^{\frac{1}{\alpha}} y f(y) F_1(y, \alpha, 0) dy, \tag{S15}$$

$$\Delta_2 = \frac{\alpha\delta(2 - \delta)}{2} \int_0^{\frac{1-\delta}{\alpha}} y^2 f(y) dy + \int_{\frac{1-\delta}{\alpha}}^{\frac{1}{\alpha}} y f(y) F_2(y, \alpha, \delta) dy, \tag{S16}$$

with,

$$F_2(y, \alpha, \delta) = \frac{\alpha y}{2} - \frac{\alpha^3 y^3}{6} - \frac{(1 - \delta)^3}{3}, \tag{S17}$$

and,

$$\Delta_3 = \frac{\alpha}{2}\int_0^{\frac{\delta}{\alpha}} y^2 f(y) F_3(y,\alpha,\delta)dy + \frac{\delta^2}{2}\left(1-\frac{2\delta}{3}\right)\int_{\frac{\delta}{\alpha}}^{\frac{1-\delta}{\alpha}} yf(y)dy + \int_{\frac{1-\delta}{\alpha}}^{\frac{1}{\alpha}} yf(y)F_4(y,\alpha,\delta)dy, \quad \text{(S18)}$$

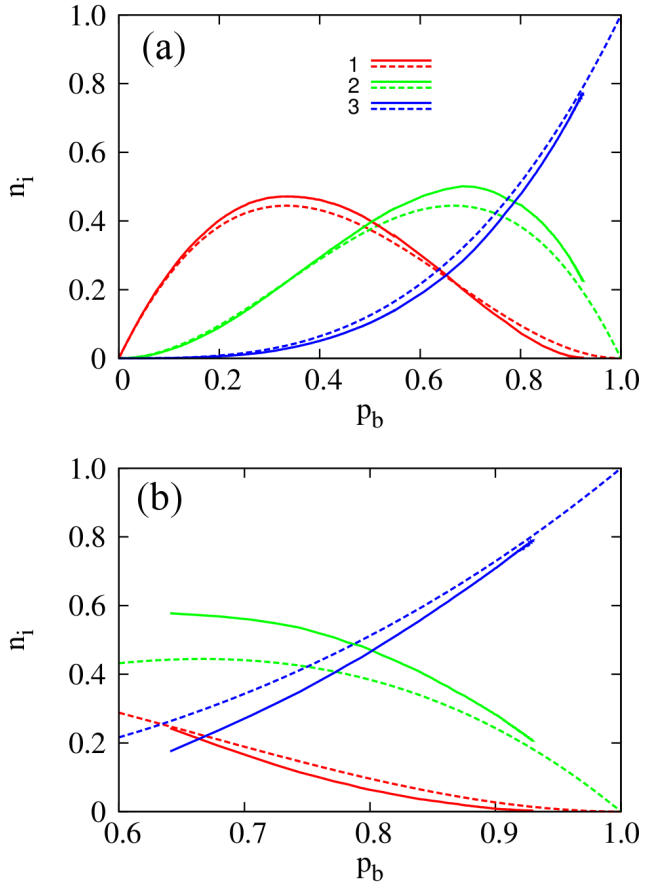

FIG. S2. Fraction of colloids with one (red), two (green), and three bonds (blue), as a function of p_b at $k_BT/\varepsilon = 0.025$ for (a) the aggregation of an initial fully disconnected suspension of patchy colloids and (b) the relaxation of a tree-like gel grown by ballistic aggregation with irreversible loopless bond formation. Dashed lines are the equilibrium values predicted by Wertheim's first-order perturbation theory. Results are averages over 100 samples for $p_b < 0.5$ and 10 samples for $p_b > 0.5$, in a cubic box of length $L = 16$, in units of particle diameter.

with,

$$F_3(y,\alpha,\delta) = 1 - \alpha y - (1-\delta)^2, \quad \text{(S19)}$$

and,

$$F_4(y,\alpha,\delta) = \frac{1}{6}(1-\alpha^3 y^3) + \frac{1}{2}(1-\alpha y)(1-\delta)^2. \quad \text{(S20)}$$

The percolation line in the ρ, T diagram (Fig. S1) is obtained by setting $p_b = \frac{1}{n-1} = \frac{1}{2}$ in Eq. (S9). The coexistence line in Fig. S1 is calculated from the equality of

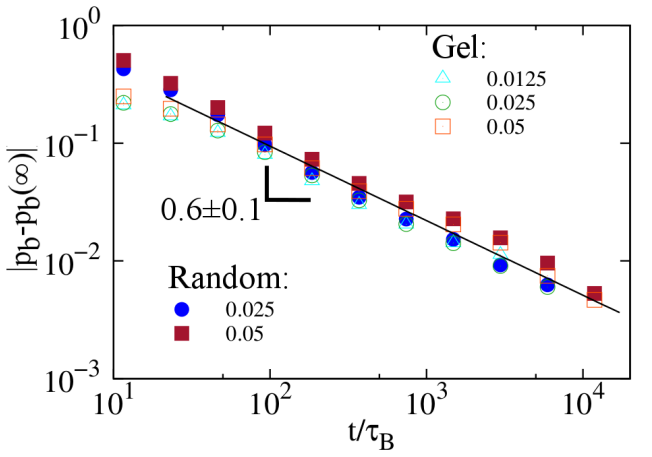

FIG. S3. Convergence of the bonding fraction to the asymptotic value, $|p_b - p_b(\infty)|$, at temperatures $k_BT/\varepsilon = \{0.0125, 0.025, 0.05\}$ starting from a singly connected tree-like gel and temperatures $k_BT/\varepsilon = \{0.025, 0.05\}$ starting from a fully disconnected suspension, where the time is in units of the Brownian time $\tau_B = \sigma^2/D_t$, where σ is the colloid diameter and D_t the diffusion coefficient. Numerical results were obtained by averaging over 10 samples in a box of length $L = 16$, in units of particle diameter.

the pressures and chemical potentials obtained from βf. The bonding fraction p_b in Fig. 1 is obtained by solving Eq. (S9), in single phase thermodynamic states. For state points in the coexistence region ($k_BT/\epsilon < 0.0678$ in Fig. 1 at $\rho = 0.2$) p_b is calculated using the so-called lever rule: $p_b(\rho,T) = p_{b,l} + x(p_{b,v} - p_{b,l})$, with $x = (\rho_l - \rho)/(\rho_l - \rho_v)$, where ρ_v and ρ_l are the coexistence vapor and liquid densities at T, and $p_{b,v}$ and $p_{b,l}$ are the bonding fractions in the coexisting vapor and liquid phases at T.

BONDING FRACTION

Figure S2 shows the fraction of colloids with one, two, and three bonds as a function of the bonding fraction. Numerically, we consider that two patches are bond if their separation is lower than 0.1σ. Equilibrium values were computed assuming no correlation between the patches,

$$\begin{aligned} n_1 &= 3p_b(1-p_b)^2, \\ n_2 &= 3p_b^2(1-p_b), \\ n_3 &= p_b^3. \end{aligned} \quad \text{(S21)}$$

Figure S2(a) shows that for initial fully disconnected suspensions these are different from the equilibrium values

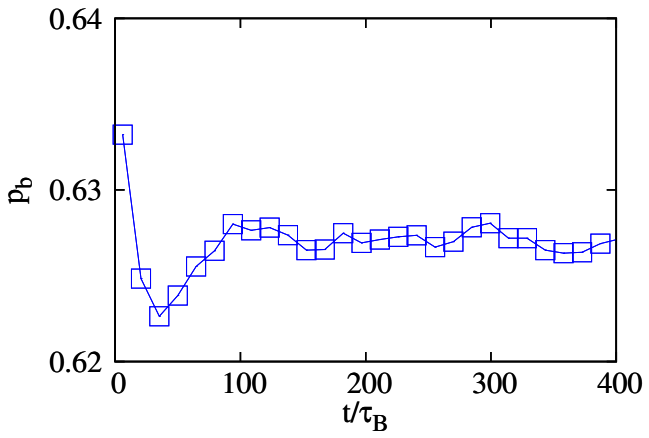

FIG. S4. Bonding fraction as a function of time at temperature $k_BT/\varepsilon = 0.075$ starting from a singly connected tree-like gel, where the initial non-equilibrium bonding fraction is close to the asymptotic one leading to the Kovacs effect observed in p_b. Numerical results were obtained by averaging over 100 samples in a box of length $L = 16$, in units of the particle diameter.

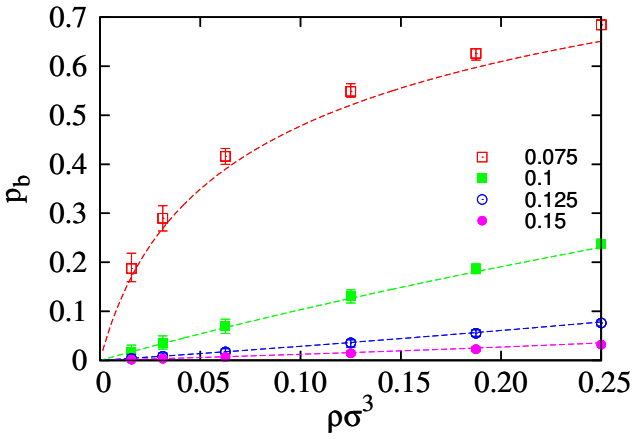

FIG. S5. Bonding fraction as a function of of the reduced density at temperatures $k_BT/\varepsilon = \{0.075, 0.1, 0.125, 0.15\}$ starting from unconnected colloidal suspensions. Numerical results were obtained by averaging over 10 samples in a box of length $L = 16$, in units of the particle diameter. The dashed lines are the equilibrium values predicted by Wertheim's first-order perturbation theory.

predicted by Wertheim's first-order perturbation theory. The same is observed in Fig. S2(b) for an initial tree-like gel. Note that the range of p_b is different as, in the latter case, one starts from a non-zero p_b.

Figure S3 reveals that the relaxation proceeds as a power law in time, with exponent 0.6 ± 0.1, which is observed for different initial conditions and temperatures below $k_BT/\varepsilon = 0.075$.

In Fig. S4 we plot the bonding fraction as a function

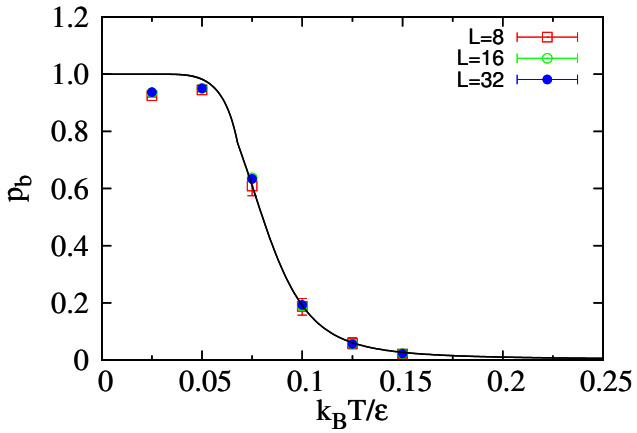

FIG. S6. Bonding fraction p_b as a function of the rescaled temperature k_BT/ε, obtained from the asymptotic extrapolation of the numerical data for systems of lateral size $L = \{8, 16, 32\}$. The solid line is the equilibrium value predicted by Wertheim's first-order perturbation theory. Numerical results were obtained by averaging over 10 samples.

of time at temperature $k_BT/\varepsilon = 0.075$ where the bonding fraction of the initial non-equilibrium branched-gel is close to the asymptotic value and a minimum is observed in the evolution of p_b. This is a signature of the Kovacs effect [8, 9], and suggests that the initial gel, while with the asymptotic value of p_b is structurally different.

Figure S5 depicts the asymptotic (numerical) and the theoretical (equilibrium) values of the bonding fraction as a function of the reduced density at temperatures $k_BT/\varepsilon = \{0.075, 0.1, 0.125, 0.15\}$ starting from unconnected colloidal suspensions. The theoretical curves are in line with the numerical results at high temperatures, but at low temperature the theory deviates from the numerical results as the density increases.

In Figure S6 we plot the asymptotic values of p_b for different system sizes showing that size effects are not significant.

COLLOIDAL STRUCTURE

In Fig. S7 we plot the radial distribution function at temperatures (a) $k_BT/\varepsilon = 0.025$ and (b) $k_BT/\varepsilon = 0.075$, and show that the long-time structure is similar when starting from a tree-like gel or a fully disconnected structure.

Finally, in Fig. S8, the intermediate scattering function is plotted at temperatures $k_BT/\varepsilon = \{0.0125, 0.025, 0.05, 0.075, 0.1, 0.125, 0.15\}$. The results show that the aging dynamics is similar after reaching both the equilibrium at high temperatures or the scale-free region at low temperatures.

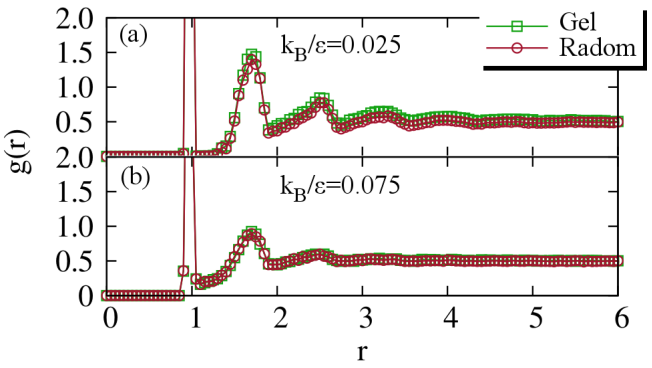

FIG. S7. Radial distribution function at temperature (a) $k_BT/\varepsilon = 0.025$ and (b) $k_BT/\varepsilon = 0.075$ starting from a (open squares) branched gel and (open circles) a random initial configuration. Numerical results were obtained by averaging over 10 samples in a box of length $L = 16$, in units of the particle diameter.

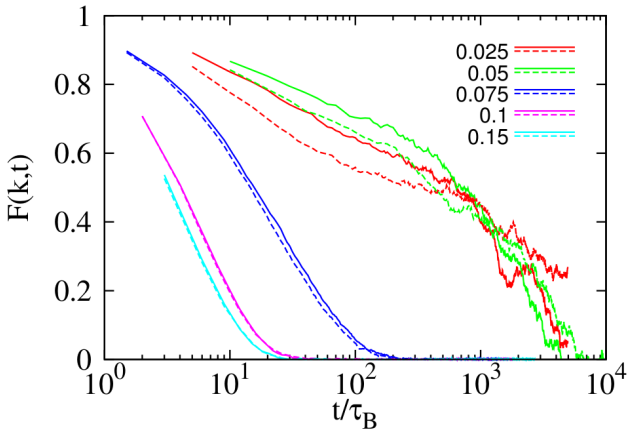

FIG. S8. Intermediate scattering function $F(k,t)$ for $k = \pi/(2\sigma)$ starting above $t/\tau_B = 100$ at high and low temperature, for both (solid) branched tree-like gel and (dashed) unconnected suspension, at temperatures $k_BT/\varepsilon = \{0.0125, 0.025, 0.05, 0.075, 0.1, 0.125, 0.15\}$. Numerical results were obtained by averaging over 10 samples at low temperature and 100 samples at high temperature, in a box of length $L = 16$, in units of the particle diameter.

[1] C. S. Dias, C. Braga, N. A. M. Araújo, and M. M. Telo da Gama, Soft Matt. **12**, 1550 (2016).
[2] O. A. Vasilyev, B. A. Klumov, and A. V. Tkachenko, Phys. Rev. E **88**, 012302 (2013).
[3] S. Plimpton, J. Comp. Phys. **117**, 1 (1995).
[4] M. G. Mazza, N. Giovambattista, H. E. Stanley, and F. W. Starr, Phys. Rev. E **76**, 031203 (2007).
[5] F. Sciortino, E. Bianchi, J. F. Douglas, and P. Tartaglia, J. Chem. Phys. **126**, 194903 (2007).
[6] J. A. Barker and D. Henderson, J. Chem. Phys. **47**, 4714 (1967).
[7] M. S. Wertheim, J. Chem. Phys. **85**, 2929 (1986).
[8] S. Mossa and F. Sciortino, Phys. Rev. Lett. **92**, 45504 (2004).
[9] A. J. Kovacs, J. J. Aklonis, J. M. Hutchinson, and A. R. Ramos, J. Polym. Sci. Part B **17**, 1097 (1979).